POLITECNICO DI TORINO
Repository ISTITUZIONALE

Vav3 Mediates Pseudomonas aeruginosa Adhesion to the Cystic Fibrosis Airway Epithelium

Original
Vav3 Mediates Pseudomonas aeruginosa Adhesion to the Cystic Fibrosis Airway Epithelium / Badaoui, M.; Zoso, A.; Idris, T.; Bacchetta, M.; Simonin, J.; Lemeille, S.; Wehrle-Haller, B.; Chanson, M.. - In: CELL REPORTS. - ISSN 2211-1247. - ELETTRONICO. - 32:1(2020). [10.1016/j.celrep.2020.107842]

Availability:
This version is available at: 11583/2845747 since: 2020-09-15T17:55:07Z

Publisher:
Elsevier B.V.

Published
DOI:10.1016/j.celrep.2020.107842

Terms of use:

This article is made available under terms and conditions as specified in the corresponding bibliographic description in the repository

Publisher copyright

(Article begins on next page)

12 October 2024

Cell Reports

Article

Vav3 Mediates *Pseudomonas aeruginosa* Adhesion to the Cystic Fibrosis Airway Epithelium

Graphical Abstract

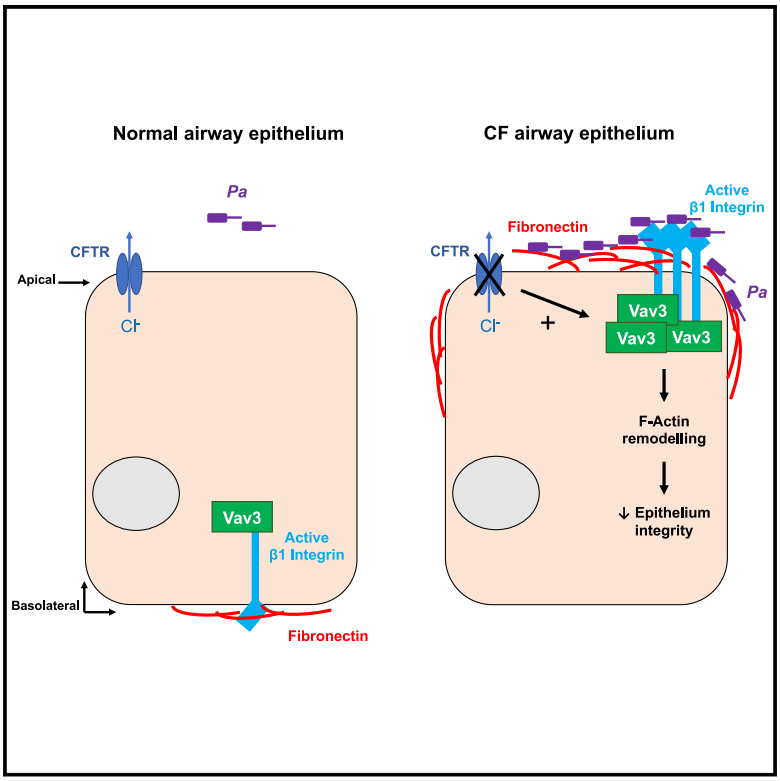

Highlights

- Vav3 is apically overexpressed in cystic fibrosis (CF) airway epithelial cells
- Vav3 promotes the luminal expression of fibronectin and active apical β1 integrin
- The ectopic complex enhances *Pseudomonas aeruginosa* adhesion to the CF epithelium
- Vav3 silencing in CF epithelial cells prevents *Pseudomonas aeruginosa* adhesion

Authors

Mehdi Badaoui, Alice Zoso, Tahir Idris, ..., Sylvain Lemeille, Bernhard Wehrle-Haller, Marc Chanson

Correspondence

marc.chanson@unige.ch

In Brief

Cystic fibrosis is characterized by chronic sinopulmonary *Pseudomonas aeruginosa* (*Pa*) infection. Badaoui et al. describe a pathway promoting luminal fibronectin deposition and apical activity of β1 integrin. This ectopic complex leads to increased *Pa* adhesion to the CF epithelium, a mechanism prevented by targeting the GTP exchange factor Vav3.

Badaoui et al., 2020, Cell Reports *32*, 107842
July 7, 2020 © 2020 The Author(s).
https://doi.org/10.1016/j.celrep.2020.107842

CellPress

Cell Reports

CellPress
OPEN ACCESS

Article

Vav3 Mediates *Pseudomonas aeruginosa* Adhesion to the Cystic Fibrosis Airway Epithelium

Mehdi Badaoui,[1,2] Alice Zoso,[1,2,4] Tahir Idris,[1,2] Marc Bacchetta,[1,2] Juliette Simonin,[1,2] Sylvain Lemeille,[3] Bernhard Wehrle-Haller,[2] and Marc Chanson[1,2,5,*]

[1]Faculty of Medicine, Department of Pediatrics, Gynecology & Obstetrics, University of Geneva, Geneva 1211, Switzerland
[2]Faculty of Medicine, Department of Cell Physiology & Metabolism, University of Geneva, Geneva 1211, Switzerland
[3]Faculty of Medicine, Department of Pathology and Immunology, University of Geneva, Geneva 1211, Switzerland
[4]Present address: Department of Mechanical and Aerospace Engineering, Politecnico di Torino, Torino 10129, Italy
[5]Lead Contact
*Correspondence: marc.chanson@unige.ch
https://doi.org/10.1016/j.celrep.2020.107842

SUMMARY

Pseudomonas aeruginosa (*Pa*) represents the leading cause of airway infection in cystic fibrosis (CF). Early airways colonization can be explained by enhanced adhesion of *Pa* to the respiratory epithelium. RNA sequencing (RNA-seq) on fully differentiated primary cultures of airway epithelial cells from CF and non-CF donors predict that *VAV3*, *β1 INTEGRIN*, and *FIBRONECTIN* genes are significantly enriched in *CF*. Indeed, Vav3 is apically overexpressed in CF, associates with active β1 integrin luminally exposed, and increases fibronectin deposition. These luminal microdomains, rich in fibronectin and β1 integrin and regulated by Vav3, mediate the increased *Pa* adhesion to the CF epithelium. Interestingly, Vav3 inhibition normalizes the CF-dependent fibronectin and β1-integrin ectopic expression, improves the CF epithelial integrity, and prevents the enhanced *Pa* trapping to the CF epithelium. Through its capacity to promote a luminal complex with active β1 integrin and fibronectin that favors bacteria trapping, Vav3 may represent a new target in *CF*.

INTRODUCTION

Cystic fibrosis (CF) is an autosomal recessive genetic disease caused by mutations in the CF transmembrane conductance regulator (*CFTR*) gene that encodes for a chloride (Cl^-) channel. The deletion of phenylalanine in position 508 (F508del-CFTR), which impairs CFTR trafficking to the plasma membrane, represents the most common mutation in the Caucasian population (Farrell, 2008; Castellani et al., 2008). Defective CFTR mainly impairs Cl^- transport, which leads to several phenotypic manifestations that affect the respiratory system. The respiratory failure and mostly the airway bacterial colonization by opportunistic pathogens determine the prognosis of the disease (Stoltz et al., 2015). *Pseudomonas aeruginosa* (*Pa*) represents the leading cause of the airway infection. Despite the effort to make the antibiotics therapy against *Pa* more widespread, the CF Foundation reported in 2017 that 30% of the European CF population and 45.7% of the American CF population are infected by *Pa* (CF Foundation [CFF] Patient Registry Annual Data Report, 2017; http://www.cff.org).

The CF epithelium is predisposed to chronic infections and the initial *Pa* infection is reported in humans at 5.2 years old (CFF Annual Data Report, 2017; http://www.cff.org), but the mechanisms involved are not fully understood. Among other hypotheses, altered mucociliary clearance due to increased mucus viscosity (Henderson et al., 2014; Boucher, 2010), decreased sphingosine-dependent killing caused by ceramide accumulation (Teichgräber et al., 2008; Grassmé et al., 2017), or acidification of the airway surface liquid that inactivate antimicrobial peptides (Smith et al., 1996; Pezzulo et al., 2012; Simonin et al., 2019) have been reported. Irreversible *Pa* adhesion to the host epithelium is the initial event that promotes airway colonization, triggering subsequent chronic infection. When attached to the epithelium surface and in the presence of a suitable local microenvironment, *Pa* initiates its growth phase, which then leads to biofilm formation (Berne et al., 2018). The adhesion process is mediated by molecular interactions between proteins expressed by piliated or non-piliated *Pa* to host cell-surface receptors or glycoconjugates (Plotkowski et al., 1991; Roger et al., 1999). There is evidence showing that OprQ and PilY1 proteins, respectively localized at the *Pa* outer membrane and pili, can directly bind to β1 integrin and fibronectin, through RGD (arginylglycylaspartic acid) peptides and fibronectin-binding domains (Rebiere-Huet et al., 2002; Arhin and Boucher, 2010; Johnson et al., 2011).

β1 integrin is a surface receptor transmitting bidirectional communication between the extracellular matrix (ECM) and the cytoskeleton (Hynes, 2002; Bouvard et al., 2013). When associated with α5 integrin, the heterodimer interacts directly with fibronectin. The integrin-mediated linkage between ECM and cytoskeleton is crucial for cell polarity establishment (Lee and Streuli, 2014). Any defect in the integrin localization can be linked to an aberrant cytoskeletal dynamic and/or ECM remodeling (Morse et al., 2014). In fact, the actin cytoskeleton rearrangement

This is an open access article under the CC BY license (http://creativecommons.org/licenses/by/4.0/).

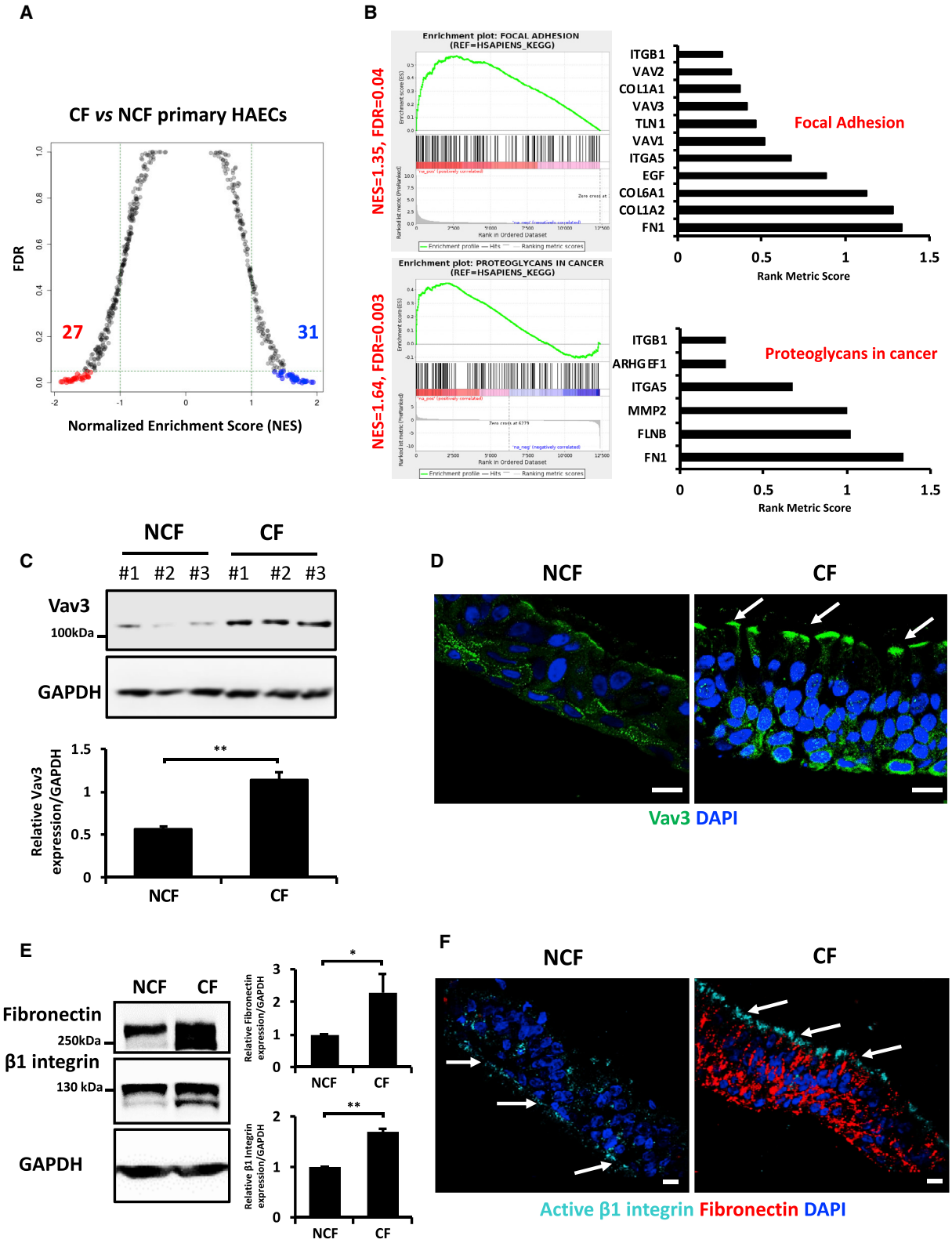

(legend on next page)

is tightly regulated by the Rho-family of small GTPases (Rho, Rac, and Cdc42; Heasman and Ridley, 2008).

The Rho-GTPases are guanine-nucleotide-binding proteins whose activity depends on their nucleotide status. Indeed, RhoA, Rac1, and Cdc42 cycle between an inactive guanosine diphosphate (GDP)-bound and an active guanosine triphosphate (GTP)-bound conformation. The GDP/GTP cycle is highly regulated by the Rho proteins activators—the guanine nucleotide exchange factors (GEFs), which catalyze the GDP exchange to GTP (Hodge and Ridley, 2016). The Vav family members Vav1, Vav2, and Vav3 belong to the GEFs (Bustelo, 2014). While Vav1 expression is limited to the hematopoietic cells, Vav2 and Vav3 are ubiquitously expressed. In addition to their capacity to regulate cytoskeleton remodeling associated to barrier stability (Hilfenhaus et al., 2018), Vav proteins are also involved in signal transduction through their functional interaction with different receptors (Moores et al., 2000). In immune cells, Vav proteins are required for integrin-dependent adhesion, spreading, polarity, and phagocytic functions (Krawczyk et al., 2002; Ardouin et al., 2003; Gakidis et al., 2004; Sindrilaru et al., 2009).

In this study, we show that in CF, Vav3 regulates the inside-out signaling that leads to the epithelium predisposition to *Pa* adhesion. Indeed, Vav3 is overexpressed in F508del-CFTR primary human airway epithelial cells (HAECs) and in the CFTR-silenced Calu-3 cell line, promoting β1 integrin and fibronectin expression at their luminal side. By regulating the cytoskeleton remodeling and its scaffold function, Vav3 controls the ectopic β1 integrin/fibronectin complex leading to the predisposition of CF airways to *Pa* adhesion. Our results indicate that Vav3 and its partners represent promising targets for *Pa* anti-adhesion therapies at the early stages of infection.

RESULTS

Vav3, β1 Integrin, and Fibronectin Are Overexpressed in CF Primary HAECs

The transcriptomic profile of fully differentiated primary HAECs from CF (N = 7) and non-CF (NCF, N = 6) donors was investigated by RNA sequencing (RNA-seq; Zoso et al., 2019). Gene set enrichment analysis (GSEA) revealed 31 upregulated pathways in CF as compared to NCF samples (Figure 1A). Interestingly, two pathways were significantly enriched in CF: "focal adhesion" (false discovery rate [FDR] = 0.04) and "proteoglycans in cancer" (FDR = 0.003); the genes contributing to these pathways are listed in Figure 1B. Interestingly, the analysis pointed to genes of the Vav's Rho-GTPase activators, β1 integrins, and components of the ECM such as fibronectin (Figure 1B). The expression of Vav family members Vav1, Vav2, and Vav3 was verified by qPCR. As shown in Figure S1A, Vav3-mRNA expression was +6.35-fold higher in CF versus NCF primary HAECs (N = 4, $p < 0.05$), whereas the expression of Vav1 and Vav2 was very low. Vav3 overexpression in CF primary HAECs was also confirmed at the protein level by western blotting (Figure 1C) and immunostaining (Figure 1D). The overexpression in CF HAECs of β1 integrin and fibronectin was also confirmed at the protein level by western blotting (Figure 1E, N = 5 CF donors and N = 4 NCF donors, $p < 0.05$). Surprisingly, confocal microscopy examination of immunostained primary HAECs revealed that Vav3 was strongly localized at the apical surface of the CF epithelium as compared to NCF primary HAECs (Figure 1D). Indeed, Vav3 will accumulate under the cilia as shown by Vav3 and acetylated α-tubulin (cilia marker) double staining in primary CF HAECs (Figure S1B). Interestingly, this ectopic localization of Vav3 was associated with an increased apical distribution of active β1 integrin (using 9EG7 antibody) in CF (Figure 1F). Fibronectin, which is a β1 integrin ligand, showed unusual accumulation at cell-cell contacts and at the apical surface of CF HAECs (Figure 1F). These results indicate that primary CF HAECs are characterized by increased expression and ectopic redistribution of fibronectin, β1 integrin and Vav3.

CFTR Silencing or Gating Mutation Induces Vav3, β1 Integrin, and Fibronectin Overexpression

To study whether there is a direct relationship among CFTR defect and the aberrant expression of Vav3, β1 integrin, and fibronectin, we silenced *CFTR* in Calu-3 airway epithelial cells (CFTR knockdown [KD]) by CRIPSR-Cas9 gene editing (Bellec et al., 2015) and Figure S2A. As compared to their controls (CTL cells), CFTR KD cells also showed enhanced expression of Vav3, β1 integrin, and fibronectin, as determined by western blotting (Figures 2A, 2C, and 2E, n = 4, $p < 0.05$). No difference was observed on Vav1- and Vav2-mRNA expression (Figure S2B, n = 4, $p > 0.05$). In addition, confocal microscopy confirmed the redistribution of these proteins at the apical side of the CFTR KD epithelium (Figures 2B, 2D, and 2F). The use of the 9EG7 antibody also demonstrated that β1 integrin is expressed as an active form, while the actin-filaments staining revealed an extracellular deposition of fibronectin at the luminal side of the epithelium.

CF is caused by different classes of CFTR mutations affecting its expression, trafficking, or channel function (Castellani et al., 2008). To test whether Vav3, fibronectin and β1 integrin overexpression is also induced by CFTR exhibiting gating-defect

Figure 1. RNA-Seq Identifies Significant Enrichment of *VAV3*, *FIBRONECTIN*, and *β1 INTEGRIN* Genes upon ΔF508 Mutation of CFTR in Primary HAECs

(A) Volcano plot transcriptomic profile of the 542 tested pathways. Blue, upregulated pathways; red, downregulated pathways. The considered misregulated pathways are FDR (false discovery rate) <0.05 and NES (normalized enrichment score) >1.

(B) Identity of the genes involved in the CF-upregulated pathways: focal adhesion and proteoglycans in cancer.

(C and D) Validation of Vav3 overexpression at the protein level by western blot (C) and immunostaining (D) in CF-versus-NCF fully differentiated primary HAECs. In (C), representative blot is shown in the top panel and quantification in the bottom panel.

(E and F) β1 integrin and fibronectin protein overexpression confirmation by western blot (N = 4 NCF and N = 5 CF; E) and their ectopic localization by confocal microscopy (F) in CF versus NCF fully differentiated primary HAECs; white arrows indicate the luminal side of the CF epithelium or the basolateral side of the NCF epithelium. In (E), representative blots are shown in the left panel and quantifications in the right panel. Scale bars: 45 μm.

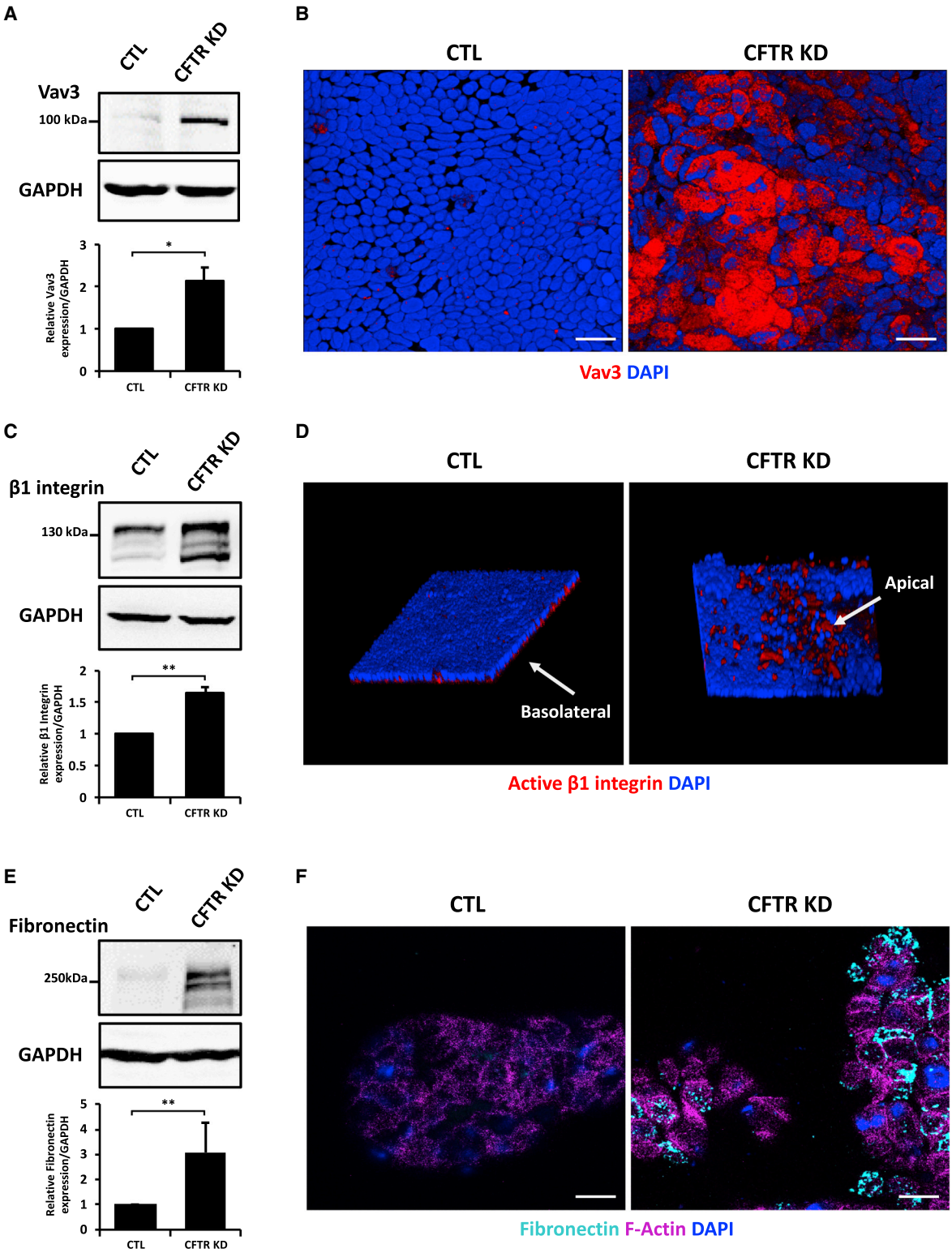

Figure 2. CFTR KD in Calu-3 Cells Promotes Vav3, Fibronectin, and β1 Integrin Overexpression at the Apical Side of the Polarized Epithelium
(A, C, and E) Representative western blot showing Vav3 (A), β1 integrin (C), and fibronectin (E) in CFTR KD versus CTL Calu-3 cells (n = 4). Representative blots are shown in the top panels and quantifications in the bottom panels.

(legend continued on next page)

mutations, we used HeLa cells stably transfected with WT CFTR (wild-type [WT]) or G551D CFTR, which represent the most prevalent CFTR gating mutation (CFF Annual Data Report, 2018; http://www.cff.org). Similar to the F508del CFTR and CFTR KD cells, G551D CFTR-HeLa cells showed increased expression of Vav3 (Figures S3A and S3B, n = 3, $p < 0.05$), fibronectin, and β1 integrin (Figures S3C–S3E, n= 3, $p < 0.05$). These results indicate that there is interplay among CFTR, Vav3, β1 integrin, and fibronectin, and that their overexpression and ectopic localization in primary CF HAECs is directly caused by CFTR defect.

Vav3 Regulates Actin Cytoskeleton Organization through Cdc42

Vav3 is a modulator of the small GTPases that control cytoskeleton network assembly through the regulation of the actin polymerization/depolymerization cycle (Hornstein et al., 2004). We next investigated actin cytoskeletal rearrangements by phalloidin staining in CFTR KD cells. Interestingly, CFTR KD cells displayed a disorganized pattern, especially at the apical side, which is associated with a higher amount of actin filament (Figure 3A). In contrast, CTL cells showed cortical filamentous actin near the cell-cell contact sites (Figure 3A). We also studied the expression of the main Rho-GTPases activated by GEFs and found enhanced expression of Cdc42 in CFTR KD cells whereas RhoA and Rac1 were not affected (Figure 3B). To investigate whether the Calu-3 actin cytoskeletal dynamics is regulated by Vav3, we generated Calu-3 cell models where Vav3 was silenced by CRISPR-Cas9 genome editing technology (Vav3 KD versus Scramble cells), without affecting Vav1 and Vav2 mRNA expression (Figure S2C). After confirmation of Cas9 (green) and Scramble/Vav3-sgRNA expression (red; Figure S4A), the efficiency of Vav3 silencing was evaluated by western blotting and immunofluorescence (Figures S4B and S4C). Silencing of Vav3 in Calu-3 cells was associated with lower amount of actin filament (Figure 3C) and decreased expression of Cdc42 (Figure 3D), results that are opposite to that observed for CFTR KD cells. RhoA and Rac1 expressions were again not affected by Vav3 silencing (Figure 3D). These findings suggest that Vav3 overexpression in CFTR KD cells led to apical disorganized actin architecture through increased Cdc42 expression.

Vav3 Regulates Fibronectin-Dependent Cell Adhesion

Remodeling of the actin cytoskeleton is critical in cellular processes like cell proliferation, adhesion, and migration. We analyzed cell growth by following cell proliferation over time (Figure S5A, $p > 0.05$) and cell cycle progression (Figure S5B, $p > 0.05$) by FACS of propidium iodide-stained cells but no difference was observed between Vav3 KD and Scramble cells. Trypan blue exclusion assay did not show any difference in cell mortality percentage after Vav3 silencing (Figure S5C, $p > 0.05$). Vav3 KD cells, however, showed slower growth rate during the first 24 h when compared to Scramble (Figure S5A). To explore this phenotype, we stained five days' cultures of Vav3 KD and Scramble cells with crystal violet. As shown in Figure S5D, crystal violet staining revealed increased spreading of Vav3-KD cells by 81% (Figure S5D, $p < 0.001$), suggesting different adhesion properties of the cells to the substrate. To address this possibility, a cell adhesion assay was performed on fibronectin or BSA-coated surfaces, BSA coating being used as negative control. Interestingly, silencing Vav3 decreased fibronectin-dependent adhesion of Calu-3 cells 1-h post-seeding (Figures 4A and 4B, $p < 0.001$). Despite this difference in early adhesion to fibronectin, silencing Vav3 did not affect Calu-3 cell migration as observed in a wound healing assay (Figures S5E and S5F). These results suggest that Vav3 is essential to mediate fibronectin-dependent adhesion in Calu-3 airway epithelial cells.

Vav3 Regulates β1 Integrin and Fibronectin Expression

ECM components modulate cell adhesion through their interactions with cell surface receptors. Fibronectin-dependent cell adhesion is mediated in part by β1 integrin (Danen et al., 2002). Therefore, we did evaluate whether decreased fibronectin-dependent adhesion of Calu3 cells induced by Vav3 silencing was associated with changes in β1 integrin functional expression. As shown in Figures 4C and 4D by western blotting, Vav3 KD cells decreased β1 integrin and fibronectin expression. In addition, β1 integrin activity was reduced by Vav3 silencing, as shown by immunostaining using the 9GE7 antibody (Figure 4E). To investigate whether Vav3 modulates β1 integrin activity through physical interaction, we carried out co-immunoprecipitation (coIP) experiments. Interestingly, Vav3 was detected after β1 integrin pull-down (Figure 4F). The same result was obtained after Vav3 pull-down (Figure 4G). Importantly, this interaction was disrupted in Vav3 KD cells as compared to controls (Figures 4F and 4G). These results indicate that Vav3, by modulating the expression/activity of β1 integrin through physical interaction, not only regulates fibronectin-dependent adhesion of Calu-3 cells, but also fibronectin expression.

Vav3, β1 integrin, and fibronectin are overexpressed at the luminal side of CF HAECs. To evaluate the consequence of increased luminal expression of fibronectin, we mimicked fibronectin accumulation by deposing fibronectin- or BSA-coated membranes for 24 h on top of the WT polarized Calu-3 cells (Figure 5A). As shown in Figures 5B and 5C, the presence of luminal fibronectin was sufficient to increase total β1 integrin expression and its recruitment to the apical side of Calu-3 cells. To determine whether Vav3 contributed to this phenotype, we performed coIP experiments using Vav3 or β1 integrin antibodies on CFTR KD versus CTL Calu-3 cells. As expected, coIP revealed that Vav3/β1 integrin complex is increased in CFTR KD cells when compared to CTL cells (Figures 5D and 5E); this observation is a direct consequence of Vav3 and β1 integrin overexpression in CF, suggesting that Vav3 regulates the fibronectin-dependent increase in β1 integrin functional expression at the luminal side of CF airway epithelial cells.

(B, D, and F) Vav3 (B), active β1-integrin (D), and fibronectin (F) localization was analyzed by confocal microscopy in the polarized CFTR KD versus CTL Calu-3 cells. Shown is the top view of representative images from 3D reconstruction of z stack confocal images; white arrows indicate the luminal side of the CF epithelium or the basolateral side of the NCF epithelium. Scale bars: 45 μm.

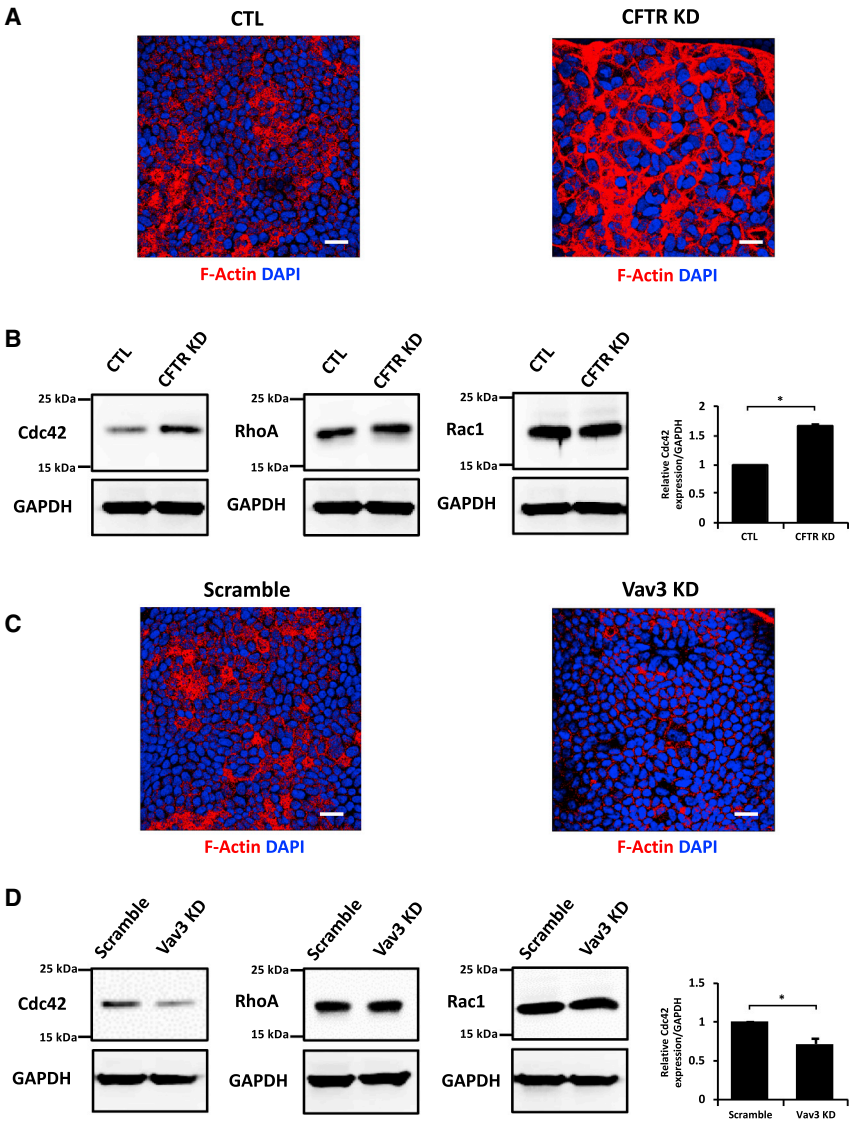

Figure 3. Vav3 Regulates Cdc42 Expression that Leads to Actin Cytoskeleton Rearrangement

(A and C) F-Actin staining with Alexa Fluor 647 phalloidin in CTL versus CFTR KD (A) and Scramble versus Vav3 KD polarized Calu-3 cells (C). Shown is the top view of representative images from 3D reconstruction of z stack confocal images. Scale bars: 25 μm.

(B and D) Cdc42, RhoA, and Rac1 expression by immunoblotting in CTL versus CFTR KD (B) and Scramble versus Vav3 KD polarized Calu-3 cells (D) (n = 3). Quantifications for Cdc42 are shown in the right panels.

Apical Secretions from CF Airway Epithelial Cells Promote Fibronectin Remodeling

Fibronectin is cleaved at specific sites by a variety of proteases to regulate its remodeling. The generated fragments act as common targets for opportunistic pathogens to mediate their adhesion and/or internalization (Henderson et al., 2011). To determine whether cleavage of luminal fibronectin is affected in CF airway epithelial cells, we collected the apical secretions from CFTR KD and CTL Calu-3 cells. To this end, the apical surface CFTR KD and CTL cells was rinsed and exposed for 24 h to a saline buffer (Figure 6). As expected, the amount of total fibronectin detected by immunoblotting was increased in the buffer collected from CFTR KD cells (Figure 6B). To evaluate protease activity of the apical secretions, 50 μg of human fibronectin (~220 kDa) was added to the conditioned buffer and samples were subjected to western blotting 1 h, 2 h, and 4 h after fibronectin addition, according to Zhang et al. (2012). Conditional buffers without added fibronectin were used as negative control (Figure 6A). As shown in Figure 6B, the CF apical secretions collected from CFTR KD cells generated more fibronectin fragments with time as compared to CTL secretions. Importantly, fragments were readily detected in conditioned buffer from CFTR KD cells without fibronectin addition (Figure 6B), confirming strong fibronectin-remodeling activity in CF. Next, glass coverslips were coated with conditioned buffers containing fragments of cleaved fibronectin, and 10^5 colony-forming units (CFUs) of the *Pa* laboratory strain PAO1 were seeded for 1 h at 37°C. Coverslips were then washed, fixed, and analyzed for PAO1 adhesion by immunostaining. As shown in Figure 6C, addition of fibronectin to the conditioned buffer from CTL cells had no effect on PAO1 adhesion. In contrast, PAO1 adhesion was markedly enhanced by the presence of fibronectin fragments generated by the CFTR KD cells apical secretions (Figure 6D, $p < 0.05$). These results suggest that increased fibronectin deposition and remodeling at the surface of CF airway epithelial cells is associated with enhanced binding of *Pa*.

Silencing Vav3 in CFTR KD Cells Restored Airway Epithelium Integrity and Prevented *Pa* Adhesion to the CF Airway Epithelium

Vav3 overexpression in CFTR KD Calu-3 cells may be critically involved in enhanced fibronectin-dependent functional expression of β1 integrin. To determine if there is a causal relationship between Vav3 and fibronectin/β1 integrin expression in CF airway epithelial cells, we generated Calu-3 cells double KD for CFTR and Vav3 (Vav3/CFTR KD cells). No compensatory mechanism on Vav1 and Vav2 mRNA expression was observed (Figure S2D, n = 3, $p > 0.05$). As shown in Figure 7A, the Scramble cells overexpress Vav3 when the CFTR is knocked-down alone. As expected, silencing Vav3 in CFTR KD cells completely inhibited the enhanced fibronectin and β1integrin expression (Figures 7A and 7B). In

CellPress
OPEN ACCESS

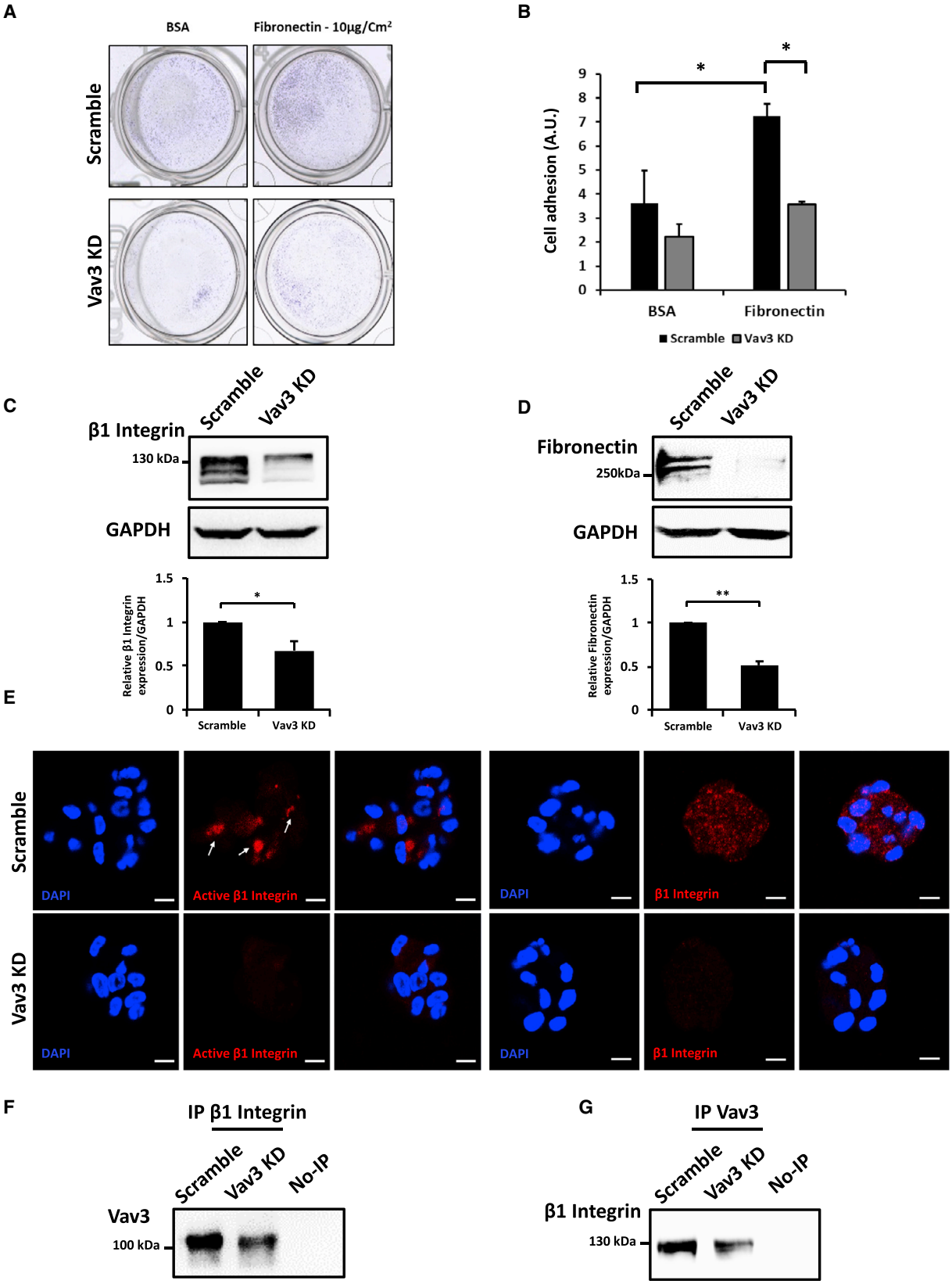

(legend on next page)

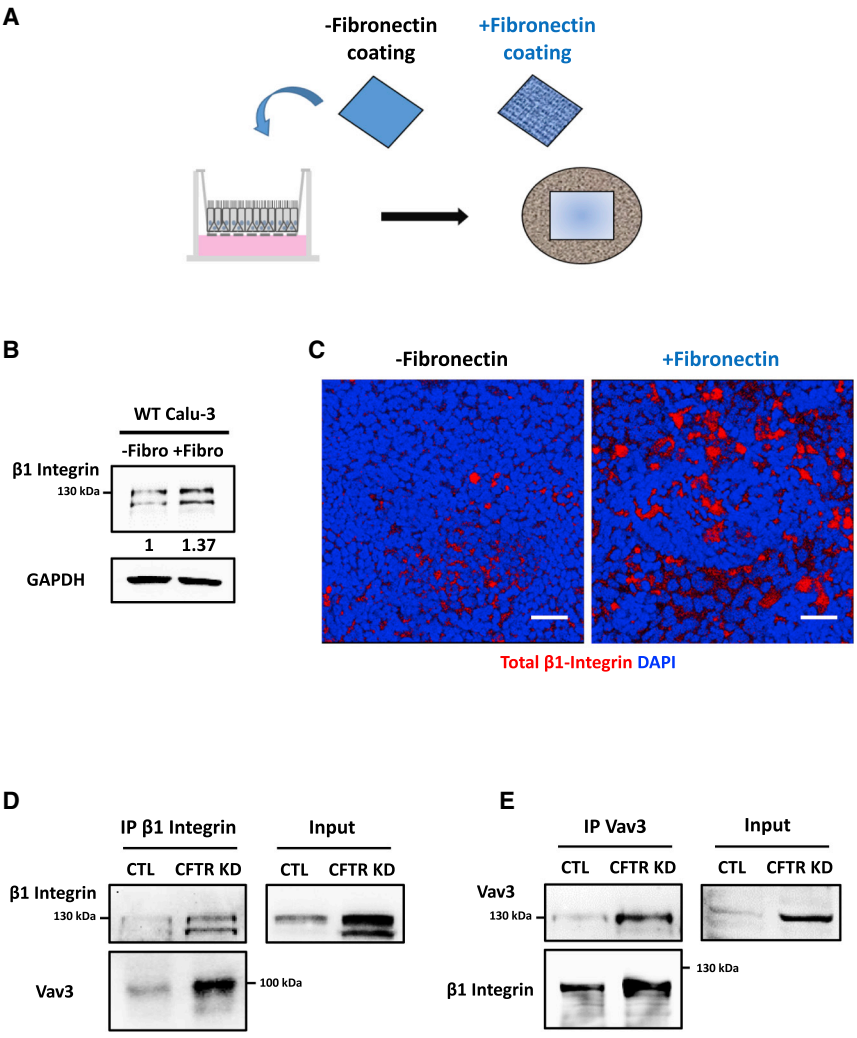

Figure 5. Apical Deposition of Fibronectin Triggers Ectopic β1 Integrin Localization

(A) Fibronectin deposition was mimicked using polyester membranes coated or not with human fibronectin at 5 μg/cm^2. The membranes were deposited on top of the WT-polarized Calu-3 cells. Fibronectin is in direct contact with the apical cells.

(B) Representative western blot showing total β1 integrin expression in the presence of the +fibronectin versus −fibronectin membranes (n = 3).

(C) Immunostaining showing total β1 integrin localization in the +fibronectin versus −fibronectin membranes. Shown is top view of representative images from 3D reconstruction of z stack confocal images. Scale bars: 40 μm.

(D and E) Representative western blot of Vav3 expression after β1 integrin immunoprecipitation (D) and β1 integrin expression after Vav3 immunoprecipitation (E) in CFTR KD versus CTL Calu-3 cells (n = 3).

addition, Vav3/CFTR KD cells exhibited normal cytoskeleton architecture (Figure S6A), reduced apical localization of β1 integrin, and absence of fibronectin at the cell surface (Figure 7C). All these modifications led to an improvement of the epithelial integrity, since the transepithelial electrical resistance (TEER) measurements revealed that Vav3 silencing in the CFTR KD restored the TEER to the same level as the CTL cells (Figure S6B).

CF is characterized by *Pa* colonization of the airways, which necessitates increased bacterial adhesion to the respiratory epithelium. This process has been shown to be regulated by membrane microdomains rich in fibronectin and β1 integrin (Hoffmann et al., 2011; Gagnière and Di Martino, 2004). Therefore, we tested whether Vav3 silencing could modulate *Pa* adhesion to CFTR-KD cells. To this end, CFTR KD, Vav3/CFTR KD cells, and their control were infected with 10^5 CFU of two laboratory strains of *Pa* (PAO1 and PAK) and two *Pa* clinical CF isolates (Liverpool Epidemic Strain B58 [LESB58] and CHA). At 1-h post infection, cells were rinsed and bacterial adhesion was analyzed by confocal microscopy using a specific antibody against *Pa* (Figures S6C–S6F). *Pa* adhesion to CFTR KD cells was increased by 2.7-, 24-, 2.6-, and 27-fold as compared to CTL cells with PAO1, PAK, LESB58, and CHA strains, respectively (Figures 7D–7G, $p < 0.05$). In contrast, after silencing Vav3 in CFTR KD cells, *Pa* adhesion was identical to their respective controls, indicating that Vav3 silencing in CFTR KD cells was sufficient to prevent the adhesion of four different *Pa* strains to the CF airway epithelium (Figures 7D–7G, $p < 0.05$). Together, our findings indicate that CFTR-dependent deregulation of Vav3 expression is critical in the cascade of events

Figure 4. Vav3 KD in Calu-3 Cells Inhibits the Fibronectin-Dependent Cell Adhesion by Reducing Fibronectin Production and β1 Integrin Functional Expression

(A and B) Calu-3 cells were seeded in 24-well plates coated with human fibronectin versus BSA. At 1-h post seeding, the cells were fixed, stained with crystal violet (A), and the cell adhesion was quantified using ImageJ (B), n = 3, *$p < 0.05$, two-way ANOVA).

(C and D) Representative western blot showing β1 integrin (C) and fibronectin (D) expression in Vav3 KD versus CTL Calu-3 cells (n = 3). Representative blots are shown in the top panels and quantifications in the bottom panels.

(E) Active and total β1 integrin immunostaining in Vav3 KD versus Scramble Calu-3 cell monolayers. White arrows indicate active β1 integrin clusters. Scale bars: 10 μm.

(F and G) Representative western blot of Vav3 expression after β1 integrin immunoprecipitation (F) and β1 integrin expression after Vav3 immunoprecipitation (G) in Vav3 KD versus Scramble Calu-3 cells (No-IP represents the negative control where the immunoprecipitant antibody was omitted; n = 3).

CellPress
OPEN ACCESS

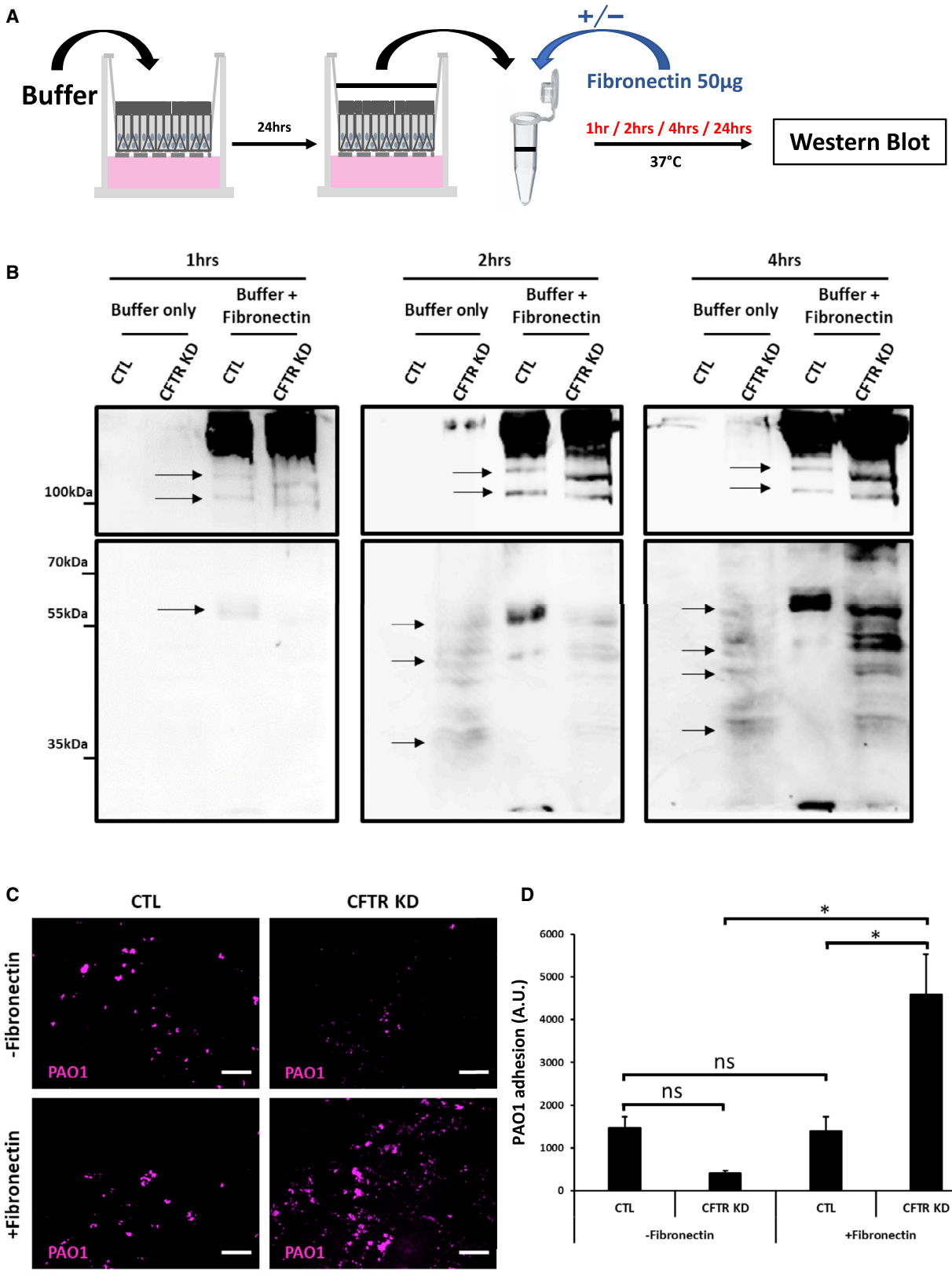

(legend on next page)

leading to ectopic redistribution of fibronectin and β1 integrin, which in turn mediates *Pa* adhesion to the CF epithelium.

DISCUSSION

Colonization of the host by opportunistic pathogens is initiated by bacterial adhesion, a critical step for the persistence of infection in *CF.* Here, we reported for the first time an inside-out signaling from the host to the extracellular microenvironment regulated by the GEF Vav3, promoting *Pa* attachment to the CF airway epithelium.

Combining RNA-seq GSEA, immunoblotting, and immunofluorescence, we observed that Vav3, fibronectin, and β1 integrinexpression is increased in well-differentiated primary HAECs from CF donors. Vav3 was mainly localized at the apical side of the CF epithelium in association with fibronectin deposition at the cell-cell interface and up to the surface. Interestingly, we also showed an ectopic accumulation of active β1 integrin at the CF cell surface, although its localization is normally confined to the basolateral membrane. These observations were confirmed in the Calu-3 cell line after specific KD of CFTR and in HeLa cells stably expressing G551D CFTR, indicating the causal relationship between the CFTR defect and abnormal expression of these proteins. Indeed, the same observations are made whether CFTR expression, trafficking, or gating is affected. Apical localization of β1 integrin was recently reported by Grassmé et al. (2017) in the upper airway epithelium through an unknown mechanism. Here, we demonstrate that the CF-dependent defect in β1 integrin expression and activity is a consequence of Vav3 overexpression.

Vav3 is a key Rho-GTPase activator leading to cytoskeletal rearrangements that regulate different cellular processes, such as cell spreading, adhesion, and migration (Li et al., 2016a; Toumaniantz et al., 2010; Carvajal-Gonzalez et al., 2009; Uen et al., 2015). In CFTR KD HAECs, Vav3 overexpression is associated with an increase in Cdc42 expression, activity (unpublished data), and higher apical F-actin dynamics. Cdc42 activity has been shown to enhance the probability of actin polymerization (Wedlich-Soldner et al., 2003) and to contribute to the establishment and the upkeep of cell polarity (Etienne-Manneville, 2004). Interestingly, Cdc42 is also described as a regulator of β1 integrin expression and localization (Reymond et al., 2012). Thus, the aberrant β1 integrin functional expression and localization observed in CF HAECs could be the consequence of Vav3-dependent Cdc42 deregulation.

It is well established that components of the ECM orientate epithelial cell polarity (Lee and Streuli, 2014) especially through fibronectin, which is required for β1 integrin recruitment and stable clustering at the plasma membrane (Roca-Cusachs et al., 2009; Tran et al., 2002). In keeping with this mechanism, we showed that Vav3, by promoting fibronectin expression and luminal deposition, induced β1 integrin apical localization. We observed that fibronectin secretion is also increased at the cell surface, an observation that is consistent with the detection of fibronectin in the secretome of the CF bronchial epithelium (Peters-Hall et al., 2015). In addition to its expression, β1 integrin activity is also increased as revealed by the 9EG7 antibody (Lenter et al., 1993), suggesting that there is a positive loop between fibronectin deposition and activation of apical β1 integrin. Thus, Vav3-dependent luminal fibronectin secretion may lead to apical β1 integrin expression that, in turn, triggers the deposition of the secreted fibronectin (Brunner et al., 2011).

We reported here for the first time that Vav3 interacts with β1 integrin. Since Vav3 could bind efficiently to ceramides via its cysteine-rich domain (CRD; Gulbins et al., 1994; Bonnefoy-Bérard et al., 1996), it is interesting to propose that interaction between the two proteins may occur in ceramide-rich regions where β1 integrin is trapped. Indeed, Vav3 may participate in β1 integrin clustering and stabilization through enhanced cortical F-actin, leading to β1 integrin locking in its active conformation (Li et al., 2016b). This interaction can be sustained by ceramide accumulation in CF, which has been shown to inhibit integrin's mobility in the membrane and increase its coupling with the actin filaments (Eich et al., 2016). Thus, our results shed new light on the central role of Vav3 in the regulation of β1 integrin high-activity conformation crucial for its avidity and binding capacity.

We found that Vav3-dependent airway epithelium remodeling enhanced *Pa* attachment through luminal fibronectin and β1 integrin. Indeed, fibronectin and β1 integrin represent common targets for many opportunistic pathogens including *Pa,* which expresses different proteins that can bind directly to integrins or fibronectin (Roger et al., 1999; Gagnière and Di Martino, 2004; Johnson et al., 2011; Hoffmann et al., 2011). Whereas previous studies reported that *Pa* induces integrin expression to mediate interaction of *Pa* with the host (Gravelle et al., 2010; Humphries et al., 2006), we showed that this process is already established in the CF airway epithelium prior to infection. Indeed, Vav3 overexpression in CF creates an extracellular environment favorable to *Pa* adhesion due to fibronectin production. Besides increasing luminal β1 integrin activity that can be used by *Pa* as a receptor to adhere, the Vav3-dependent deposition of fibronectin associated with CF apical secretions may generate a specific profile and higher number of fibronectin fragments to promote *Pa* adhesion. There is ample evidence that the CF lung disease is characterized by a protease/antiprotease imbalance (Voynow et al., 2008; McKelvey et al., 2019) caused by increased neutrophil serine protease activity, bacterial proteases, and modified airway epithelial secretions. As predicted in our RNA-seq

Figure 6. CF Apical Secretions Promote Fibronectin Cleavage Leading to the Increased Susceptibility to *Pa* Attachment

(A) The CF apical secretions were collected using saline buffer for 24 h. Fifty micrograms of human fibronectin were added to the conditioned buffer for 1 h, 2 h, 3 h, 4 h, and 24 h at 37°C (n = 3).

(B) Representative western blot showing fibronectin expression and the generated fibronectin fragments by the CF secretions 1 h, 2 h, and 4 h after fibronectin addition.

(C) The generated fibronectin fragments after 24 h were used to coat coverslips that were then infected with 10^5 CFU of PAO1 at 37°C in a 5%-CO_2 atmosphere. At 1-h post infection, PAO1 adhesion was analyzed by immunostaining using a PAO1-specific antibody and quantified using ImageJ (n = 2, *$p < 0.05$, two-way ANOVA). Scale bars: 20 μm.

CellPress
OPEN ACCESS

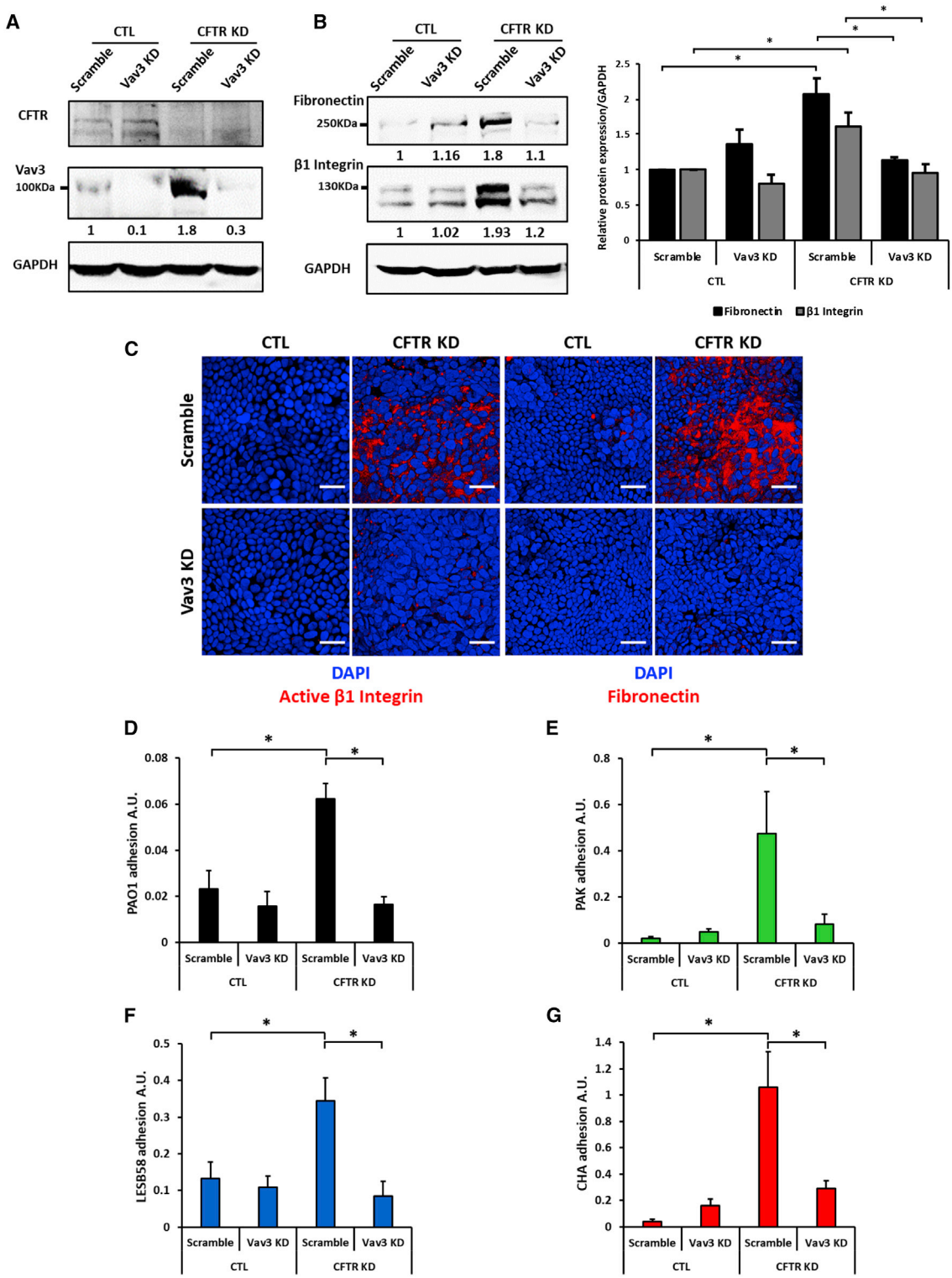

Figure 7. Vav3 Inhibition Prevents *Pa* Adhesion to the CFTR KD Cells by Reducing Fibronectin Deposition and β1 Integrin Activity

(A and B) Representative western blot of CFTR (A), Vav3 (A), fibronectin (B), and β1 integrin (B) expression in CFTR KD, Vav3 KD, and CFTR/Vav3 KD Calu-3 cells, compared to their respective controls (n = 3).

(legend continued on next page)

analysis on CF primary HAECs (Figure 1B) and previously reported for CF bronchial epithelial cells (Peters-Hall et al., 2015; Gaggar et al., 2011), deregulation in the expression of metalloproteases (MMPs) could favor *Pa* adhesion by cleavage and remodeling of fibronectin. Although the precise mechanism awaits confirmation, the CF fibronectin cleavage may generate soluble fragments that would bridge *Pa* to the β1 integrin, leading to irreversible adhesion to the cell surface. Thus, CFTR-dependent Vav3 overexpression may predispose the CF airway epithelium to infection.

Importantly, Vav3 silencing in CFTR KD cells normalized fibronectin and β1 integrin expression, which was sufficient to prevent adhesion of *Pa* to the epithelial cell surface. We believe that targeting Vav3 may present multiple benefits at different steps of *Pa* colonization, by maintaining the epithelium integrity through normalized cytoskeleton remodeling, cancelling the CF epithelium predisposition to *Pa* adhesion, and, finally, by restoring bacterial killing. In this context, Grassmé et al. (2017) recently demonstrated that inactivating luminal β1 integrin enhanced sphingosine-dependent killing of *Pa* in CF HAECs and CF mice. Indeed, β1 integrin downregulates acid ceramidase expression, resulting in accumulation of ceramide and consequent reduction of surface sphingosine, a lipid that kills bacteria (Seitz et al., 2015). Thus, our results point to Vav3 as a key player between CFTR defect and β1 integrin/fibronectin accumulation to the cell surface with dramatic consequences on *Pa* adhesion and killing. The mechanism leading to Vav3 overexpression in CF remains unknown. It is noteworthy that β1 integrin expression is increased and apically exposed during normal airway epithelium reparation, a process associated with higher fibronectin production (Hérard et al., 1996; Roger et al., 1999). This repair process was associated with de-differentiation and loss of polarity of airway epithelial cells (Hérard et al., 1996). Since CFTR may contribute to airway epithelial repair and regeneration (Barbry et al., 2019), it is tempting to speculate that Vav3 deregulation in CF is a consequence of abnormal airway epithelial cell differentiation.

In conclusion, our data describe a new protein complex induced at the luminal side of airway epithelial cells when *CFTR* is mutated or KD; it is composed of fibronectin, active β1 integrin, and the cytoskeleton regulator Vav3, and represents a key player in this ectopic communication between the host and its luminal environment. This complex predisposed the CF epithelium to *Pa* early adhesion, which may represent the "decisive phase" for airway colonization. The development of new anti-adhesion therapies represents an important challenge and alternative strategy for efficient treatment of acute and chronic infections (Krachler and Orth, 2013). Thus, Vav3-dependent inside-out signaling could be potentially exploited in the research for novel antivirulence targets in CF.

STAR★METHODS

Detailed methods are provided in the online version of this paper and include the following:

- KEY RESOURCES TABLE
- RESOURCE AVAILABILITY
  - Lead Contact
  - Materials Availability
  - Data and Code Availability
- EXPERIMENTAL MODEL AND SUBJECT DETAILS
  - Primary human airway epithelial cells and Calu-3 cell line
- METHOD DETAILS
  - RNA-seq
  - Gene set enrichment analyses
  - Adhesion assay
  - Cell growth and mortality
  - Cell migration
  - Cell cycle analysis (fluorescence-activated cell sorting)
  - Western blot
  - Co-immunoprecipitation
  - Confocal microscopy
  - RNA extraction, RT-PCR and qPCR
  - Transepithelial electrical resistance measurements (TEER)
  - Pseudomonas aeruginosa adhesion assay
- QUANTIFICATION AND STATISTICAL ANALYSIS

SUPPLEMENTAL INFORMATION

Supplemental Information can be found online at https://doi.org/10.1016/j.celrep.2020.107842.

ACKNOWLEDGMENTS

We thank the Faculty of Medicine Core Facilities (University of Geneva): Flow Cytometry, Bioimaging, Genomics Platform (iGE3) and READS (Readers, Assay Development & Screening) unit for their excellent technical support. We also thank Pr. Christian Van Delden, Dr. Thilo Köhler and Alexandre Luscher (Department of Microbiology and Molecular Medicine, University of Geneva, Switzerland) for kindly providing *Pa* strains. We thank Pr. Claude Férec and Dr. Pascal Trouvé (Department of "Génétique, Génomique Fonctionnelle et Biotechnologies," University of Brest, France) for the kind gift of WT-CFTR and G551D-CFTR HeLa cells. This work was supported by the Swiss National Science Foundation, Switzerland (310030–172909).

AUTHOR CONTRIBUTIONS

M.C. and M. Badaoui designed the experiments, performed data interpretation, and prepared the manuscript; M. Badaoui., A.Z., and T.I. performed experiments; M. Bacchetta performed culture and cryosectioning of primary HAECs; S.L. performed bioinformatic analyses; J.S. supplied bacteriology advisement; and B.W.-H. provided β1 integrin and fibronectin tools. All authors reviewed the manuscript.

(C) Top view from 3D reconstruction of z stack confocal images showing active β1 integrin and fibronectin expression and localization in CFTR KD, Vav3 KD, and CFTR/Vav3 KD Calu-3 cells, compared to their respective controls. Scale bars: 20 μm.

(D–G) *Pa* adhesion to the CFTR KD, Vav3 KD, and CFTR/Vav3 KD Calu-3 cells, compared to their respective controls. Polarized Calu-3 cells were apically infected with 10^5 CFU of PAO1 (D), PAK (E), LESB58 (F), and CHA (G) at 37°C in a 5%-CO_2 atmosphere. At 1-h post-infection, the adherent *Pa* strains were analyzed by immunostaining using anti-*Pa* antibody and quantified using ImageJ ($n = 3$, $^*p < 0.05$, two-way ANOVA).

DECLARATION OF INTERESTS

The authors declare no competing interests.

Received: November 28, 2019
Revised: April 13, 2020
Accepted: June 9, 2020
Published: July 7, 2020

REFERENCES

Ardouin, L., Bracke, M., Mathiot, A., Pagakis, S.N., Norton, T., Hogg, N., and Tybulewicz, V.L. (2003). Vav1 transduces TCR signals required for LFA-1 function and cell polarization at the immunological synapse. Eur. J. Immunol. *33*, 790–797.

Arhin, A., and Boucher, C. (2010). The outer membrane protein OprQ and adherence of Pseudomonas aeruginosa to human fibronectin. Microbiology *156*, 1415–1423.

Barbry, P., Cavard, A., Chanson, M., Jaffe, A.B., and Plasschaert, L.W. (2019). Regeneration of airway epithelial cells to study rare cell states in cystic fibrosis. J. Cyst. Fibros. *19*, S42–S46.

Bellec, J., Bacchetta, M., Losa, D., Anegon, I., Chanson, M., and Nguyen, T.H. (2015). CFTR inactivation by lentiviral vector-mediated RNA interference and CRISPR-Cas9 genome editing in human airway epithelial cells. Curr Gene Ther *15*, 447–459. https://doi.org/10.2174/1566523215666150812115939.

Berne, C., Ellison, C.K., Ducret, A., and Brun, Y.V. (2018). Bacterial adhesion at the single-cell level. Nat. Rev. Microbiol. *16*, 616–627.

Bonnefoy-Bérard, N., Munshi, A., Yron, I., Wu, S., Collins, T.L., Deckert, M., Shalom-Barak, T., Giampa, L., Herbert, E., Hernandez, J., et al. (1996). Vav: function and regulation in hematopoietic cell signaling. Stem Cells *14*, 250–268. https://doi.org/10.1002/stem.140250.

Boucher, R.C. (2010). Bronchiectasis: a continuum of ion transport dysfunction or multiple hits? Am J Respir Crit Care Med *181*, 1017–1019. https://doi.org/10.1164/rccm.201002-0284ED.

Bouvard, D., Pouwels, J., De Franceschi, N., and Ivaska, J. (2013). Integrin inactivators: balancing cellular functions in vitro and in vivo. Nat. Rev. Mol. Cell Biol. *14*, 430–442.

Brunner, M., Millon-Frémillon, A., Chevalier, G., Nakchbandi, I.A., Mosher, D., Block, M.R., Albigès-Rizo, C., and Bouvard, D. (2011). Osteoblast mineralization requires beta1 integrin/ICAP-1-dependent fibronectin deposition. J. Cell Biol. *194*, 307–322.

Bustelo, X.R. (2014). Vav family exchange factors: an integrated regulatory and functional view. Small GTPases *5*, 9.

Carvajal-Gonzalez, J.M., Mulero-Navarro, S., Roman, A.C., Sauzeau, V., Merino, J.M., Bustelo, X.R., and Fernandez-Salguero, P.M. (2009). The dioxin receptor regulates the constitutive expression of the vav3 proto-oncogene and modulates cell shape and adhesion. Mol. Biol. Cell *20*, 1715–1727.

Castellani, C., Cuppens, H., Macek, M., Jr., Cassiman, J.J., Kerem, E., Durie, P., Tullis, E., Assael, B.M., Bombieri, C., Brown, A., et al. (2008). Consensus on the use and interpretation of cystic fibrosis mutation analysis in clinical practice. J. Cyst. Fibros. *7*, 179–196.

Danen, E.H., Sonneveld, P., Brakebusch, C., Fassler, R., and Sonnenberg, A. (2002). The fibronectin-binding integrins alpha5beta1 and alphavbeta3 differentially modulate RhoA-GTP loading, organization of cell matrix adhesions, and fibronectin fibrillogenesis. J. Cell Biol. *159*, 1071–1086.

Eich, C., Manzo, C., de Keijzer, S., Bakker, G.J., Reinieren-Beeren, I., García-Parajo, M.F., and Cambi, A. (2016). Changes in membrane sphingolipid composition modulate dynamics and adhesion of integrin nanoclusters. Sci. Rep. *6*, 20693.

Etienne-Manneville, S. (2004). Cdc42—the centre of polarity. J. Cell Sci. *117*, 1291–1300.

Farrell, P.M. (2008). The prevalence of cystic fibrosis in the European Union. J. Cyst. Fibros. *7*, 450–453.

Gaggar, A., Hector, A., Bratcher, P.E., Mall, M.A., Griese, M., and Hartl, D. (2011). The role of matrix metalloproteinases in cystic fibrosis lung disease. Eur. Respir. J. *38*, 721–727. https://doi.org/10.1183/09031936.00173210.

Gagnière, H., and Di Martino, P. (2004). alpha5beta1 integrins and fibronectin are involved in adherence of the Pseudomonas aeruginosa ER97314 clinical strain to A549 cells. Folia Microbiol. (Praha) *49*, 757–762.

Gakidis, M.A., Cullere, X., Olson, T., Wilsbacher, J.L., Zhang, B., Moores, S.L., Ley, K., Swat, W., Mayadas, T., and Brugge, J.S. (2004). Vav GEFs are required for beta2 integrin-dependent functions of neutrophils. J. Cell Biol. *166*, 273–282.

Grassmé, H., Henry, B., Ziobro, R., Becker, K.A., Riethmuller, J., Gardner, A., Seitz, A.P., Steinmann, J., Lang, S., Ward, C., et al. (2017). Beta1-integrin accumulates in cystic fibrosis luminal airway epithelial membranes and decreases sphingosine, promoting bacterial infections. Cell Host Microbe *21*, 707–718 e708.

Gravelle, S., Barnes, R., Hawdon, N., Shewchuk, L., Eibl, J., Lam, J.S., and Ulanova, M. (2010). Up-regulation of integrin expression in lung adenocarcinoma cells caused by bacterial infection: in vitro study. Innate Immun. *16*, 14–26.

Gulbins, E., Coggeshall, K.M., Baier, G., Telford, D., Langlet, C., Baier-Bitterlich, G., Bonnefoy-Berard, N., Burn, P., Wittinghofer, A., and Altman, A. (1994). Direct stimulation of Vav guanine nucleotide exchange activity for Ras by phorbol esters and diglycerides. Mol. Cell. Biol. *14*, 4749–4758.

Guzmán, C., Bagga, M., Kaur, A., Westermarck, J., and Abankwa, D. (2014). ColonyArea: an ImageJ plugin to automatically quantify colony formation in clonogenic assays. PLoS ONE *9*, e92444.

Heasman, S.J., and Ridley, A.J. (2008). Mammalian Rho GTPases: new insights into their functions from in vivo studies. Nat. Rev. Mol. Cell Biol. *9*, 690–701.

Henderson, A.G., Ehre, C., Button, B., Abdullah, L.H., Cai, L.-H., Leigh, M.W., DeMaria, G.C., Matsui, H., Donaldson, S.H., Davis, C.W., et al. (2014). Cystic fibrosis airway secretions exhibit mucin hyperconcentration and increased osmotic pressure. J Clin Invest *124*, 3047–3060. https://doi.org/10.1172/JCI73469.

Henderson, B., Nair, S., Pallas, J., and Williams, M.A. (2011). Fibronectin: a multidomain host adhesin targeted by bacterial fibronectin-binding proteins. FEMS Microbiol. Rev. *35*, 147–200.

Hérard, A.L., Pierrot, D., Hinnrasky, J., Kaplan, H., Sheppard, D., Puchelle, E., and Zahm, J.M. (1996). Fibronectin and its alpha 5 beta 1-integrin receptor are involved in the wound-repair process of airway epithelium. Am. J. Physiol. *271*, L726–L733.

Hilfenhaus, G., Nguyen, D.P., Freshman, J., Prajapati, D., Ma, F., Song, D., Ziyad, S., Cuadrado, M., Pellegrini, M., Bustelo, X.R., and Iruela-Arispe, M.L. (2018). Vav3-induced cytoskeletal dynamics contribute to heterotypic properties of endothelial barriers. J. Cell Biol. *217*, 2813–2830.

Hodge, R.G., and Ridley, A.J. (2016). Regulating Rho GTPases and their regulators. Nat. Rev. Mol. Cell Biol. *17*, 496–510.

Hoffmann, C., Ohlsen, K., and Hauck, C.R. (2011). Integrin-mediated uptake of fibronectin-binding bacteria. Eur. J. Cell Biol. *90*, 891–896.

Hornstein, I., Alcover, A., and Katzav, S. (2004). Vav proteins, masters of the world of cytoskeleton organization. Cell. Signal. *16*, 1–11.

Humphries, J.D., Byron, A., and Humphries, M.J. (2006). Integrin ligands at a glance. J. Cell Sci. *119*, 3901–3903.

Hynes, R.O. (2002). Integrins: bidirectional, allosteric signaling machines. Cell *110*, 673–687.

Johnson, M.D., Garrett, C.K., Bond, J.E., Coggan, K.A., Wolfgang, M.C., and Redinbo, M.R. (2011). Pseudomonas aeruginosa PilY1 binds integrin in an RGD- and calcium-dependent manner. PLoS ONE *6*, e29629.

Krachler, A.M., and Orth, K. (2013). Targeting the bacteria-host interface: strategies in anti-adhesion therapy. Virulence *4*, 284–294.

Krawczyk, C., Oliveira-dos-Santos, A., Sasaki, T., Griffiths, E., Ohashi, P.S., Snapper, S., Alt, F., and Penninger, J.M. (2002). Vav1 controls integrin

clustering and MHC/peptide-specific cell adhesion to antigen-presenting cells. Immunity *16*, 331–343.

Lee, J.L., and Streuli, C.H. (2014). Integrins and epithelial cell polarity. J. Cell Sci. *127*, 3217–3225.

Lenter, M., Uhlig, H., Hamann, A., Jenö, P., Imhof, B., and Vestweber, D. (1993). A monoclonal antibody against an activation epitope on mouse integrin chain beta 1 blocks adhesion of lymphocytes to the endothelial integrin alpha 6 beta 1. Proc. Natl. Acad. Sci. USA *90*, 9051–9055.

Li, M., Zhang, S., Wu, N., Wu, L., Wang, C., and Lin, Y. (2016a). Overexpression of miR-499-5p inhibits non-small cell lung cancer proliferation and metastasis by targeting VAV3. Sci. Rep. *6*, 23100.

Li, Z., Lee, H., and Zhu, C. (2016b). Molecular mechanisms of mechanotransduction in integrin-mediated cell-matrix adhesion. Exp. Cell Res. *349*, 85–94.

McKelvey, M.C., Weldon, S., McAuley, D.F., Mall, M.A., and Taggart, C.C. (2019). Targeting proteases in cystic fibrosis lung disease: paradigms, progress, and potential. Am. J. Respir. Crit. Care Med. *201*, 141–147.

Moores, S.L., Selfors, L.M., Fredericks, J., Breit, T., Fujikawa, K., Alt, F.W., Brugge, J.S., and Swat, W. (2000). Vav family proteins couple to diverse cell surface receptors. Mol. Cell. Biol. *20*, 6364–6373.

Morse, E.M., Brahme, N.N., and Calderwood, D.A. (2014). Integrin cytoplasmic tail interactions. Biochemistry *53*, 810–820.

Peters-Hall, J.R., Brown, K.J., Pillai, D.K., Tomney, A., Garvin, L.M., Wu, X., and Rose, M.C. (2015). Quantitative proteomics reveals an altered cystic fibrosis in vitro bronchial epithelial secretome. Am. J. Respir. Cell Mol. Biol. *53*, 22–32.

Pezzulo, A.A., Tang, X.X., Hoegger, M.J., Abou Alaiwa, M.H., Ramachandran, S., Moninger, T.O., Karp, P.H., Wohlford-Lenane, C.L., Haagsman, H.P., van Eijk, M., et al. (2012). Reduced airway surface pH impairs bacterial killing in the porcine cystic fibrosis lung. Nature *487*, 109–113.

Plotkowski, M.C., Chevillard, M., Pierrot, D., Altemayer, D., Zahm, J.M., Colliot, G., and Puchelle, E. (1991). Differential adhesion of Pseudomonas aeruginosa to human respiratory epithelial cells in primary culture. J. Clin. Invest. *87*, 2018–2028.

Rebière-Huët, J., Guérillon, J., Pimenta, A.L., Di Martino, P., Orange, N., and Hulen, C. (2002). Porins of Pseudomonas fluorescens MFO as fibronectin-binding proteins. FEMS Microbiol. Lett. *215*, 121–126.

Reymond, N., Im, J.H., Garg, R., Vega, F.M., Borda d'Agua, B., Riou, P., Cox, S., Valderrama, F., Muschel, R.J., and Ridley, A.J. (2012). Cdc42 promotes transendothelial migration of cancer cells through β1 integrin. J. Cell Biol. *199*, 653–668.

Roca-Cusachs, P., Gauthier, N.C., Del Rio, A., and Sheetz, M.P. (2009). Clustering of alpha(5)beta(1) integrins determines adhesion strength whereas alpha(v)beta(3) and talin enable mechanotransduction. Proc. Natl. Acad. Sci. USA *106*, 16245–16250.

Roger, P., Puchelle, E., Bajolet-Laudinat, O., Tournier, J.M., Debordeaux, C., Plotkowski, M.C., Cohen, J.H., Sheppard, D., and de Bentzmann, S. (1999). Fibronectin and alpha5beta1 integrin mediate binding of Pseudomonas aeruginosa to repairing airway epithelium. Eur. Respir. J. *13*, 1301–1309.

Seitz, A.P., Grassmé, H., Edwards, M.J., Pewzner-Jung, Y., and Gulbins, E. (2015). Ceramide and sphingosine in pulmonary infections. Biol. Chem. *396*, 611–620.

Simonin, J., Bille, E., Crambert, G., Noel, S., Dreano, E., Edwards, A., Hatton, A., Pranke, I., Villeret, B., Cottart, C.H., et al. (2019). Airway surface liquid acidification initiates host defense abnormalities in cystic fibrosis. Sci. Rep. *9*, 6516.

Sindrilaru, A., Peters, T., Schymeinsky, J., Oreshkova, T., Wang, H., Gompf, A., Mannella, F., Wlaschek, M., Sunderkötter, C., Rudolph, K.L., et al. (2009). Wound healing defect of Vav3-/- mice due to impaired beta2-integrin-dependent macrophage phagocytosis of apoptotic neutrophils. Blood *113*, 5266–5276.

Smith, J.J., Travis, S.M., Greenberg, E.P., and Welsh, M.J. (1996). Cystic fibrosis airway epithelia fail to kill bacteria because of abnormal airway surface fluid. Cell *85*, 229–236.

Srinivasan, B., Kolli, A.R., Esch, M.B., Abaci, H.E., Shuler, M.L., and Hickman, J.J. (2015). TEER measurement techniques for in vitro barrier model systems. J. Lab. Autom. *20*, 107–126.

Stoltz, D.A., Meyerholz, D.K., and Welsh, M.J. (2015). Origins of cystic fibrosis lung disease. N. Engl. J. Med. *372*, 1574–1575.

Teichgräber, V., Ulrich, M., Endlich, N., Riethmüller, J., Wilker, B., De Oliveira-Munding, C.C., van Heeckeren, A.M., Barr, M.L., von Kürthy, G., Schmid, K.W., et al. (2008). Ceramide accumulation mediates inflammation, cell death and infection susceptibility in cystic fibrosis. Nat Med *14*, 382–391. https://doi.org/10.1038/nm1748.

Toumaniantz, G., Ferland-McCollough, D., Cario-Toumaniantz, C., Pacaud, P., and Loirand, G. (2010). The Rho protein exchange factor Vav3 regulates vascular smooth muscle cell proliferation and migration. Cardiovasc. Res. *86*, 131–140.

Tran, H., Pankov, R., Tran, S.D., Hampton, B., Burgess, W.H., and Yamada, K.M. (2002). Integrin clustering induces kinectin accumulation. J. Cell Sci. *115*, 2031–2040.

Uen, Y.H., Fang, C.L., Hseu, Y.C., Shen, P.C., Yang, H.L., Wen, K.S., Hung, S.T., Wang, L.H., and Lin, K.Y. (2015). VAV3 oncogene expression in colorectal cancer: clinical aspects and functional characterization. Sci. Rep. *5*, 9360.

Voynow, J.A., Fischer, B.M., and Zheng, S. (2008). Proteases and cystic fibrosis. Int. J. Biochem. Cell Biol. *40*, 1238–1245.

Wedlich-Soldner, R., Altschuler, S., Wu, L., and Li, R. (2003). Spontaneous cell polarization through actomyosin-based delivery of the Cdc42 GTPase. Science *299*, 1231–1235.

Zhang, X., Chen, C.T., Bhargava, M., and Torzilli, P.A. (2012). A comparative study of fibronectin cleavage by MMP-1, -3, -13, and -14. Cartilage *3*, 267–277.

Zoso, A., Sofoluwe, A., Bacchetta, M., and Chanson, M. (2019). Transcriptomic profile of cystic fibrosis airway epithelial cells undergoing repair. Sci. Data *6*, 240.

CellPress
OPEN ACCESS

STAR★METHODS

KEY RESOURCES TABLE

REAGENT or RESOURCE	SOURCE	IDENTIFIER
Airway Epithelial Cells		
NCF Primary HAECs	Epithelix Sàrl	EP01MD
CF Primary HAECs	Epithelix Sàrl	EP07MD
Calu-3 cell line	ATCC	HTB-55
CRISPR Products		
Cas9 Lentiviral particles	GeneCopoeia	LPP-CP-LVC9NU-10-100-cs
Scramble sgRNA Lentiviral particles	GeneCopoeia	LPPCCPCTR01L03-100-cs
Vav3 sgRNA Lentiviral particles	GeneCopoeia	LPPHCP000983L03-1-50-01
Antibodies		
Vav3	Sigma-Millipore	Cat# 07-464, RRID:AB_310637
Total β1 integrin	Cell Signaling	Cat# 4706, RRID:AB_823544
Active β1 integrin (Clone 9EG7)	BD Biosciences	Cat# 553715, RRID:AB_395001
Acetyl-alpha Tubulin	ThermoFisher	Cat# 32-2700, RRID:AB_2533073
Rac1	Cell Biolabs	Cat# 240106
RhoA	Cell Biolabs	Cat# 240302
Cdc42	Cell Biolabs	Cat# 240201
CFTR (Clone 24.1)	R&D Systems	Cat# MAB25031, RRID:AB_2260673
CFTR mAb570	Cystic Fibrosis Foundation	Cat# 570
CFTR mAb596	Cystic Fibrosis Foundation	Cat# 596
Pseudomonas aeruginosa	Abcam	Cat# ab68538, RRID:AB_1270071
GAPDH	Millipore	Cat# MAB374, RRID:AB_2107445
Fibronectin	Polyclonal antisera against human plasma fibronectin (Gift from Dr B. Wehrle-Haller)	Clone 1801
Goat anti-Rabbit HRP	Sigma	Cat# A8275, RRID:AB_258382
Goat anti-Mouse HRP	Sigma	Cat# A5278, RRID:AB_258232
Alexa Fluor 647 Phalloidin	ThermoFisher	Cat# A22287, RRID:AB_2620155
Alexa Fluor 568 goat anti-rabbit (H+L)	ThermoFisher	Cat# A-11011, RRID:AB_143157
Alexa Fluor 647 goat anti-rabbit (H+L)	ThermoFisher	Cat# A-21245, RRID:AB_2535813
Alexa Fluor 568 goat anti-mouse (H+L)	ThermoFisher	Cat# A-11031, RRID:AB_144696
Alexa Fluor 647 goat anti-mouse (H+L)	ThermoFisher	Cat# A-21236, RRID:AB_141725
Oligonucleotides		
qPCR primers	Microsyth	See qPCR section
Other reagents		
MEM-Glutamax	GIBCO®	41090-028
MucilAir Culture Medium	Epithelix Sàrl	EP04MM
Non-Essential Amino Acids	Bioconcept	5-13K00-H
HEPES	GIBCO®	15630-056
Sodium pyruvate 100X	GIBCO®	11360-039
Fetal Bovine Serum (FBS)	GIBCO®	10270-106
Penicillin / Streptomycin / Fungizone ®	Bioconcept	4-02F00-H
Hygromycin	InvivoGen	ant-hg-1
Puromycin	InvivoGen	ant-pr-1
Polybrene	Santa Cruz Biotechnology	sc-134220
Fibronectin Human Protein, Plasma	Invitrogen	33016015

(*Continued on next page*)

Continued

REAGENT or RESOURCE	SOURCE	IDENTIFIER
BSA	Applichem	A1391
Versene	GIBCO®	15040-033
Trypsin-EDTA 10X	GIBCO®	15400-054
PBS	GIBCO®	14190-094
Crystal violet	Sigma	C0775
Trypan blue 0.4%	Invitrogen	T10282
Ribonuclease A	Sigma	R5500
Propidium Iodide	Sigma	P4170
Nonidet-P40	Applichem	A1694
cOmplete *Protease Inhibitor* Cocktail	Roche	04693124001
Pierce BCA protein assay kit	ThermoFisher	23228
Porablot NCP nitrocellulose membrane	Macherey-Nagel	741280
Tween® 20	Sigma	P2287
HRP substrate Immobilon Western	Millipore	WBKLS0500
Protein A/G magnetic beads mix Pureproteome	Millipore	LSKMAGAG02
Paraformaldehyde (PFA)	Sigma	158127
Triton 100X	Sigma	T8787
DAPI	Applichem	A4099
RNeasy mini kit	QIAGEN	74106
PowerUp SYBR Green Master Mix	Appliedbiosystems	A2574

RESOURCE AVAILABILITY

Lead Contact

Further information and requests for resources and reagents should be directed to and will be fulfilled by the Lead Contact, Pr. Marc Chanson (marc.chanson@unige.ch).

Materials Availability

All unique/stable reagents generated in this study are available from the Lead Contact without restriction.

Data and Code Availability

This study did not generate any datasets or codes.

EXPERIMENTAL MODEL AND SUBJECT DETAILS

Primary human airway epithelial cells and Calu-3 cell line

Well-differentiated primary Human Airway Epithelial Cells (HAECs) isolated form bronchial biopsies were purchased from Epithelix Sàrl (Switzerland). The donor's clinical informations are provided in Table S1. The primary HAECs were cultured in MucilAir Culture Medium from Epithelix Sàrl (Switzerland).

The male HAEC line Calu-3 was purchased from the American Type Culture Collection (ATCC® HTB-55) and cultured in Minimum Essential Medium (MEM) GlutaMAX Supplement containing, 1% non-essential amino acids (NEAA) 100X, 1% HEPES 1M, 1% sodium pyruvate 100X, 10% heat-inactivated Fetal Bovine Serum (FBS) and antibiotic/antimycotic Solution (Penicillin/Streptomycin/Amphotericin B) at 37°C in humidified 5% CO_2 atmosphere. Calu-3 cells were seeded on Petri dishes or coverslips for monolayers, while polarized Calu-3 cells are obtained by seeding 1.75×10^5 cells in 0.33 cm^2 surface/0.4 μm pore polyester membrane inserts (Costar®). At 100% of confluency, the Calu-3 cells were polarized at Air-Liquid Interface (ALI) for minimum 15 days for all cell lines expect WT Calu-3 cell line, which was maintained at ALI for minimum 10 days. HeLa cells expressing WT-CFTR or G551D-CFTR were cultures in Dulbecco's Modified Eagle Medium (DMEM) High glucose L-Glutamine containing, 1% non-essential amino acids (NEAA) 100X, 1% HEPES 1M, 10% heat-inactivated Fetal Bovine Serum (FBS) and antibiotic/antimycotic Solution (Penicillin/Streptomycin/Amphotericin B) at 37°C in humidified 5% CO_2 atmosphere.

The Vav3 KD Calu-3 cells were obtained using lentiviral particles (GeneCopoeia) coding for Cas9 nucleases (promoter: EF1a, reporter: EGFP, resistance marker: hygromycin, Cat.No.: LPP-CP-LVC9NU-10-100-cs), Scramble sgRNA (promoter: U6, reporter:

mCherry, resistance marker: puromycin, Cat.No.: LPPCCPCTR01L03-100-cs) or Vav3 sgRNA (promoter: U6, reporter: mCherry, resistance marker: puromycin, Cat.No.: LPPHCP000983L03-1-50-01).

The cells were seeded at $6x10^4$ and infected with Cas9/Vav3 sgRNA versus Cas9/Scramble sgRNA lentivirus in presence of Polybrene (Sigma) for 4hrs at 37°C in humidified 5% CO_2 atmosphere. After Hygromycin and Puromycin selection, the double positive cells for mCherry and GFP were sorted by FACS.

METHOD DETAILS

RNA-seq

RNA isolation and RNA-seq were performed on well-differentiated HAECs from 7 CF versus 6 NCF donors as previously described (Zoso et al., 2019).

Gene set enrichment analyses

All annotated pathways for *Homo sapiens*, *Mus musculus*, *Rattus norvegicus*, *Danio rerio*, *Sus scrofa* and *Saccharomyces cerevisiae* available on WikiPathways database (http://www.wikipathways.org/index.php/WikiPathways) were used to generate gene sets, as well as the KEGG metabolic pathways (KEGG http://www.genome.jp/kegg/) relative to GRCh38.80. Genes were ranked by their calculated fold-changes (decreasing ranking). A gene set analysis using the GSEA package Version 2.2 from the Broad Institute (MIT, Cambridge, MA) was used to analyze the pattern of differential gene expression between the CF versus NCF groups. Gene set permutations were performed 1000 times for each analysis. The Normalized Enrichment Score (NES) was calculated for each gene set. GSEA results with a nominal FDR < 0.05 and abs(NES) > 1 were considered significant.

Adhesion assay

To test the fibronectin-dependent adhesion, 6 or 24 well plates were coated with human fibronectin (GIBCO) or BSA (Bovine Serum Albumin Fraction V, used as negative control) at $5\mu g/cm^2$ for 1hr at 37°C. During the coating, the Calu-3 cells were detached using Versene solution (GIBCO®, 0.2 g EDTA(Na_4) per liter of Phosphate Buffered Saline (PBS) which is a gentle non-enzymatic cell dissociation method in order to avoid any cleavage of the adhesive proteins. Cells were seeded on the coated plates at a density of 10^5 and cultured at 37°C 5% CO_2. 1hr and 2hrs post-seeding, the adherent cells were washed with PBS, fixed and stained using 0.1% Crystal violet, 10% methanol solution. The cell adhesion was quantified using the ImageJ plugin "ColonyArea" (Guzmán et al., 2014).

Cell growth and mortality

Cell growth and mortality were assessed by Trypan Blue exclusion assay. 10^5 cells of Vav3KD and Scramble Calu-3 cells were grown on 35 mm Petri dishes. 24hrs, 48hrs, 72hrs and 96hrs post-seeding the cells were detached by trypsin treatment and diluted in Trypan Blue. Cell count was performed 8 times per sample from 3 independent experiments. Viable cells were represented as cell number ± SEM while the cell mortality was represented as the percentage ± SEM of dead cells relative to the total cell number.

Cell migration

Calu-3 cells were grown in 2 wells silicone culture-insert (Ibidi, Cat. No. 80209) that was removed after confluency, making 500 μm cell-free gap necessary for reproducible experiments. The wound healing was followed 6hrs, 14hrs, 16hrs and 18hrs post-insert removal, 5 images per sample were taken using through AMG EVOS fluorescence microscope and the wound area was measured using the ImageJ macro "MRI Wound Healing Tool" (http://dev.mri.cnrs.fr/projects/imagej-macros/wiki/Wound_Healing_Tool). Data were represented as an average of the wound area ± SEM.

Cell cycle analysis (fluorescence-activated cell sorting)

Calu-3 cells (Vav3KD versus CTL) were cultured in medium described above. Before confluency the cells were detached, rinsed with PBS and centrifuged at 200 g for 7min. The cells were re-suspended in PBS-EDTA solution to avoid aggregates formation and fixed with ice-cold 70% ethanol at 4°C. Once fixed, pellets ($\approx 10^6$ cells) were washed again, treated with ribonuclease A (RNase A) for 30 min at 37°C and stained with 5-20 ug of Propidium Iodide overnight at room temperature. Samples were then protected from light and the cell cycle distribution was analyzed using BD Accuri C6 flow cytometer (BD Biosciences).

Western blot

Proteins were extracted from Calu-3 cells and HeLa cells using Nonidet-P40 lysis buffer (150 mM Sodium chloride, 50 mM Tris (pH 8.0), 1% NP-40 and Roche cOmplete Protease Inhibitor Cocktail). The cell lysates were centrifuged at 10 000 g for 15min at 4°C and the protein concentration was quantified with Pierce BCA protein assay kit. 10ug of proteins were separated in denaturing SDS-PAGE, transferred into Porablot NCP nitrocellulose membrane and blocked for 1hr at RT using 3% BSA in PBS-Tween (0.01) buffer. The primary antibodies are listed in the Key Resources Table and were incubated with the membranes overnight at +4°C with agitation. GAPDH was used as loading control. After primary antibody fixation, the membranes were washed with PBS-Tween buffer and

followed by horseradish peroxidase-coupled secondary antibody incubation. Proteins were finally detected using the chemiluminescent HRP substrate Immobilon Western (Millipore, Cat. No. WBKLS0500) and quantified with Quantity One Analyses Software (Biorad).

Co-immunoprecipitation

To investigate the physical interaction between Vav3 and β1 integrin, 300μl of lysis buffer containing 500μg of the extracted proteins from Vav3-KD, CFTR-KD Calu-3 cell monolayers and their respective controls were incubated for the precleaning step with 50μl of Protein A/G magnetic beads mix Pureproteome for 2hrs at +4°C. Next, the supernatant was incubated with Vav3 or β1 integrin specific antibody overnight at +4°C and 50μl of Protein A/G magnetic beads mix Pureproteome were added to the mix (protein and antibody) for 1hr at +4°C leading to the immunoprecipitation of the complex. The beads were then collected, washed and denatured with Laemmli buffer at 95°C. The immunoprecipitated proteins are finally analyzed by western blot. The No-IP condition represents the negative control where no immunoprecipitant antibody was added.

Confocal microscopy

Frozen cryosections from CF and NCF well differentiated primary HAECs were immediately fixed in 4% Paraformaldehyde solution (PFA) for 30min on ice and permeabilized for 15min at RT with 0.2% Triton 100X buffer. Polarized Vav3-KD, CFTR-KD or Vav3/KD Calu-3 cells and their respective controls were fixed using 4% PFA for 20 min at RT and permeabilized for 15min at RT with 0.2% Triton 100X buffer. The non-specific sites were blocked by PBS-BSA 3% solution for 30 min at RT and the slides were then incubated with primary antibody recognizing the proteins of interest (Table 2) at +4°C overnight. After PBS washing, secondary anti-rabbit, anti-mouse or anti-rat secondary AlexaFluor® 568/647 antibody was applied for 1hr at RT for the detection of the different proteins, while DAPI was used for the nuclear counterstaining. The fluorescence images and Z stacks were acquired with LSM700 confocal microscope and ZEN software (ZEISS). The images were analyzed using ZEN and ImageJ software.

RNA extraction, RT-PCR and qPCR

Total RNA was extracted from polarized Calu-3 cells with RNeasy mini kit (QIAGEN, Cat. No.74106). RNA concentration and purity were verified by Nanodrop 2000 (ThermoFisher) spectrophotometer. Genomic DNA was removed using gDNA wipeout buffer for 2min at 42°C and cDNA was synthetized with the QuantiTect Reverse Transcription Kit. qPCR was performed with PowerUp SYBR Green Master Mix using the StepOnePlus Real-Time PCR system. Vav1, Vav2 and Vav3 mRNA expression is represented as absolute value ($2^{-\Delta Ct}$) normalized to GAPDH/18S expression. The following primers (Microsynth AG) were used: Vav1 5′-TCTGCCCAAGATGGAGGTGTTTCA-3′ (forward) and 5′- TTCGTGAGCTCCACAATGTCTCCA −3′ (reverse); Vav2 5′- AAGCC TGTGCTGACCTTCCAG −3′ (forward) and 5′- GTGTAGTCGATCTCCCGGGAT −3′ (reverse); Vav3 5′- TCTGAAAGGAGATGCACA CAGT −3′ (forward) and 5′- ACTGTGTGCATCTCCTTTCAGA −3′ (reverse); GAPDH 5′- TGGTATCGTGGAAGGACTCATGAC −3′ (forward) and 5′- ATGCCAGTGACGTTCCCGTTCAGC −3′ (reverse); 18 s 5′- GTAACCCGTTGAACCCCATT −3′ (forward) and 5′-CCATCCAATCGGTAGTAGCG −3′ (reverse).

Transepithelial electrical resistance measurements (TEER)

Transepithelial electrical resistance (TEER) measurements were made on polarized Calu-3 cells grown on transwell filters using the epithelial voltmeter (EVOM, World Precision Instruments, Inc). TEER was measured in PBS according to Srinivasan et al., (2015). Resistance measurements were performed in duplicate for each filter and expressed as $\Omega.cm^2$.

Pseudomonas aeruginosa adhesion assay

Pa adhesion was studied using four different strains, the laboratory strains *PAO1* and *PAK* and two clinical CF isolates, *LESB58* (hypervirulent clinical Cystic Fibrosis isolate) and *CHA* (mucoid clinical Cystic Fibrosis isolate) strains. All the strains were grown in Lysogeny Broth (LB) medium. Polarized Calu-3 cells, from which antibiotics were previously removed from the cell culture medium 24hrs before bacterial infection, were infected apically with 10μl of PAO1 suspension containing a final inoculum of 10^5 CFU at 37°C in 5% CO_2 atmosphere. 1hr post-infection the cells were rinsed with PBS and fixed with PFA for 15 min at room temperature. After the permeabilization step, the adherent *Pa* was detected using *Pa* specific antibody and analyzed by confocal imaging. 10 images per transwell were taken and quantified using ImageJ software.

QUANTIFICATION AND STATISTICAL ANALYSIS

Values are represented as mean ± SEM. The statistical tests were realized using SigmaStat software (Systat Software, Inc.). The differences between two groups were analyzed by Student's t test or the nonparametric Mann-Whitney Rank Sum test. While the differences between more than two groups were tested using the Two-Way analysis of variance (ANOVA) followed by Holm-Sidak post hoc tests. $p < 0.05$, $p < 0.01$, $p < 0.001$ are considered significant and expressed as *, **, ***, respectively.